International Conferences on Recent Advances in Geotechnical Earthquake Engineering and Soil Dynamics

1991 - Second International Conference on Recent Advances in Geotechnical Earthquake Engineering & Soil Dynamics

12 Mar 1991, 10:30 am - 12:00 pm

Cyclic Undrained Tests Along Constant Axial Stress on Hollow Cylinder

O. Hameury
Ecole Nationale des Travaux Publics de l'Etat, France

T. Doanh
Ecole Nationale des Travaux Publics de l'Etat, France

Recommended Citation

Hameury, O. and Doanh, T., "Cyclic Undrained Tests Along Constant Axial Stress on Hollow Cylinder" (1991). *International Conferences on Recent Advances in Geotechnical Earthquake Engineering and Soil Dynamics*. 12.
https://scholarsmine.mst.edu/icrageesd/02icrageesd/session01/12

Proceedings: Second International Conference on Recent Advances in Geotechnical Earthquake Engineering and Soil Dynamics, March 11-15, 1991, St. Louis, Missouri, Paper No. 1.64

Cyclic Undrained Tests Along Constant Axial Stress on Hollow Cylinder

O. Hameury, T. Doanh
Ecole Nationale des Travaux Publics de l'Etat. Laboratoire Géomatériaux. Vaulx en Velin. France

SYNOPSIS: Cyclic hollow cylinder tests have been performed on sand and clay under undrained conditions. In order to point out the effects of the rotation of principal axes, a constant axial stress is maintained during the application of torsional shear.
On this stress path, the behaviour of the two materials is studied in terms of stress-strain relationship, pore pressure, failure criterion and also rotation of strain principal axes.

INTRODUCTION

The rotation of principal axes is a fundamental aspect of soils, specially when seismic sollicitations are applied. This phenomenon can be simulated in laboratory using hollow cylinder specimens where the application of a torque provides a continuous rotation of the principal stress directions.

Cyclic torsional shear tests have been performed in the past by Towhata and Ishihara (1985) on different stress paths, including pure torsional shear or cyclic test with circular rotation of the principal stress axes; and Hicher (1987) on Ko-consolidated Edgar clay.

Our tests, on Hostun RF sand and also kaolinite P300, have been achieved on particular loading paths: first triaxial compression and then cyclic torsional loadings, both under undrained conditions. Two of them will be presented here.

EXPERIMENTAL SETUPS

The two different hollow cylinders have been developed in the Geomaterials Laboratory (LGM) by Golcheh (1986) and Kharchafi (1988).

1-The total stress path.
The loading path can be described in the plane torsional shear-axial deviator in three parts:

- first the sample is consolidated isotropically in the cell, then we apply an undrained triaxial compression which will constitute the starting point of the cyclic tests;
- then the tests are continued with two-way cyclic torsional shear, under undrained conditions, with a constant strain rate (low for clay), while the axial stress and the cell pressure are kept constant;
- if the failure doesn't occur yet, the tests end with a monotonic shear loading or a triaxial extension.

2-Tests description.
From the tests which have been achieved on both kaolinite and sand, three specific ones have been excerpted:

Nature	σ_c' kPa	$\sigma_a-\sigma_\theta$ kPa	τ_{max} kPa	α_σ °
Clay AK05	500	50	50	32
Clay AK06	500	50	00	
Sand SA0407	200	150	100	27

The test named AK05 has only three torsional cycles; it will be compared to reference test AK06 which hasn't undergown the cycles. Five cycles have been accomplished on test SA0407 (dense sand, e_o=0.68).

TESTS RESULTS

1-Effective stress path.
The application of a torsional shear not only reorients the principal stress directions, but also leads the sample to a three-dimensional stress state. This state can be represented in the three-dimensional axes, (τ, p', $\sigma_a-\sigma_\theta$), figure 0 .

For more accuracy, we will use two planes: (τ,p') and the projection of the effective stress path on the octahedral plane. As the effective mean pressure changes during the tests, this projection is obtained by mutiplying the deviator stress by the ratio between the initial mean pressure and the current mean pressure.

The monotonic test on clay (AK06) provides a linear effective stress path, and the failure happens at 39.5° of stress rotation (b=0.41). Then the torque is unloaded and the path becomes non linear. For the cyclic test AK05 (fig 1c), we superimpose the experimental data with the Lade's failure criterion, obtained with isotropical consolidated samples whose friction angle in triaxial compression is 21°.

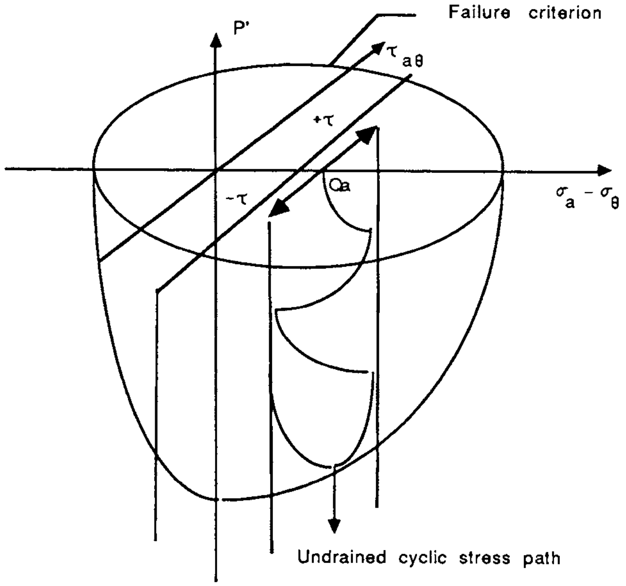

Figure 0: Effective stress path.

2-The evolution of pore pressure.
The test performed on clay shows us (fig 1b) that the pore pressure always increases during the cycles, but this augmentation decreases with the number of cycles. The material is still contractant (by analogy with the drained behaviour). The evolution of pore pressure changes when the accumulation of pore pressure oversteps the maximal level reached by the monotonic test.

Though the pore pressure increases during the three cycles, it almost follows the monotonic curve. Beneath a level of shear strain or stress, which hasn't yet been determined exactly, the torsional loading succeeding to the cycles erases the memory of clay.
The same behaviour is observed in the π-plane (fig 1c), and also in the plane (τ,p') (fig 1d) where tests AK05 and AK06 have been plotted together.

The test SA0407 conducted on dense sand reveals a global increasing of the pore pressure (fig 2b), though for each cycle it increases and then decreases, phenomenon due to the contractancy and dilatancy of dense sand under drained conditions. The differences between each cycle tend to diminish and stabilization seems to occur during the last cycles.

For all the tests, the accumulation of pore pressure induces a decreasing of the mean effective pressure during the torsion shear cycles; fig 1d and 2d reveal a progressive shift towards the low mean effective pressure. However, p' can never tend to zero (fig 1d, 2d). So following this stress path, the liquefaction cannot happen. On tests AK05 and SA0407 one observes a stabilization of the torsional cycles, different for sand and clay: the low level of torque applied to the kaolinite doesn't allow the generation of hysteresis loops in the (τ,p') plane which are obtained on sand.

The Lade's failure criterion has also been plotted in this representation. It enforces the experimental results: the constant axial stress prevents the liquefaction of the material. On the opposite, a triaxial extension conducted on SA0407 after the cyclic loadings proved that liquefaction is possible on loose sand only by unloading the axial stress.

3-Shear stress-shear strain relationship (fig 2a, 2b).
Corresponding to the level of torsional shear stress, two behaviours have been observed on both clay and sand. First the phenomenon of stabilization for low amplitudes: the cyclic and permanent shear strains are stable; on the other hand these strains increase significantly with the amount of cycles, for those which develop a great level of torsional stress.

Finally, test SA0407 (fig 2a) clearly shows that the stress-strain curves move to the left (negative strains), which may be due to the effects of the first torsional loading.

4-Rotation of principal axes.
The combinaison of constant axial stress and torque provides a continuous rotation of stress and strain principal axes. Fig 2c represents the angle of principal stress directions α_σ versus the angle of principal strain axes α_ε, which are given by:

$$\tan(2\alpha_\sigma) = \frac{2\tau}{(\sigma_a-\sigma_\theta)} \text{ and } \tan(2\alpha_\varepsilon) = \frac{2\gamma}{(\varepsilon_a-\varepsilon_\theta)}$$

As the tests are stress-controlled, the amplitude of α_σ still remains constant. However, we see that α_ε decreases during the cyclic loadings. So we can say that this loading path induces a reorientation of the strain principal axes, from high rotations to low angles with the vertical direction. In other words, the axial strain becomes more and more significant during the torsional cycles.

For several tests, the failure occured with shear bands far less inclined than for monotonic tests.

CONCLUSIONS.

The cyclic torsional shear tests lead to the following experimental conclusions:
1-The pore pressure globally accumulates during the cycles, even with dense sand, whatever the level of the torsional shear stress is;
2-There is a threshold of stabilization of the behaviour. Over this level, the two-way torsional cycles bring the sample to failure;
3-The coupling effects between axial and shear strains are emphasized by the torsional cycles; the strain state at failure is approximatively the same as the state given by a classical triaxial compression;
4-The mean effective pressure decreases during the cycles, but the sample never liquefy because of the initial axial deviator applied by the previous triaxial compression;
5-The test AK05 proved that the strength of kaolinite is not modified by a few number of cycles or after the stabilization of the behaviour. An isotropic criterion, for example Lade's one, can fairly well represent the shear stress of sand or kaolinite.

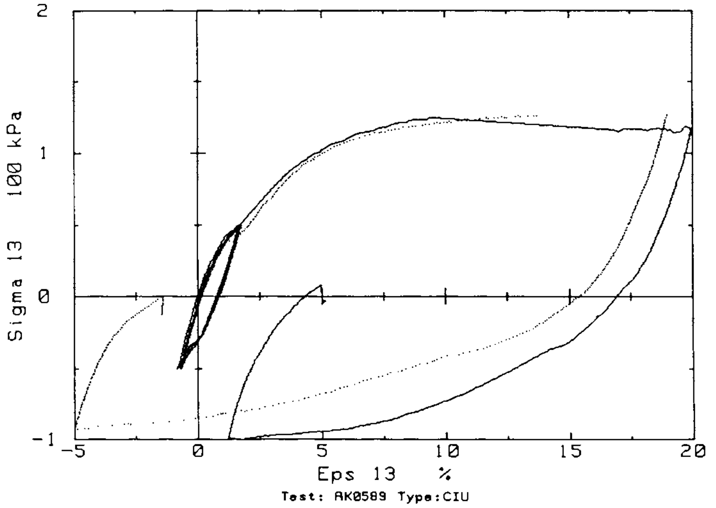

Figure 1a: Cyclic results of clay

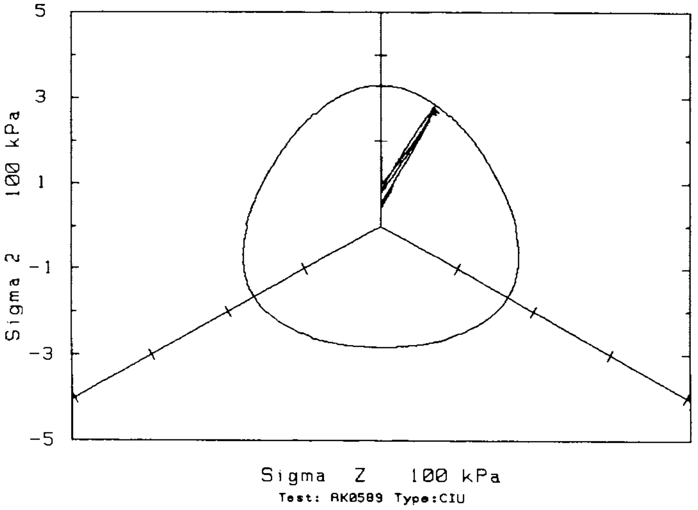

Figure 1c: Cyclic results of clay

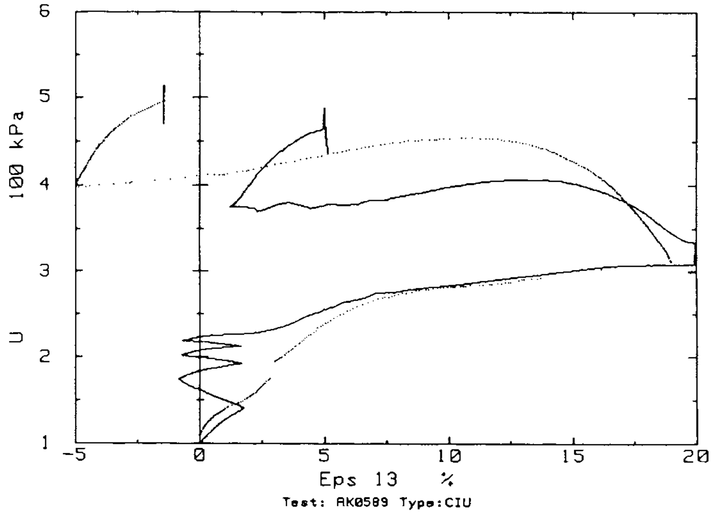

Figure 1b: Cyclic results of clay

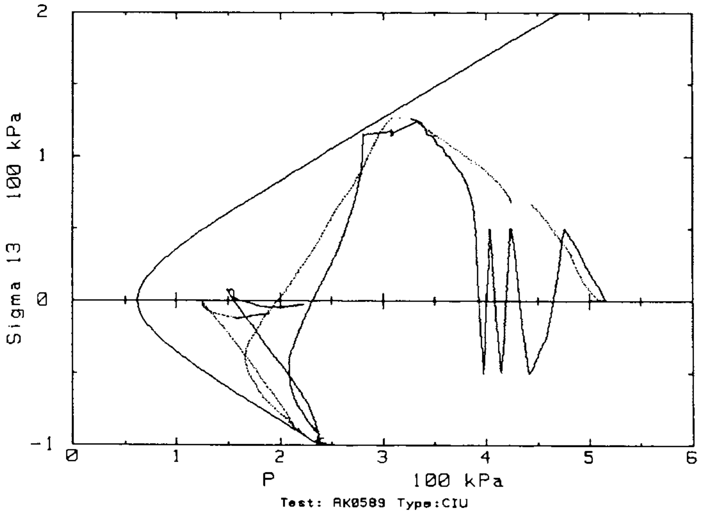

Figure 1d: Cyclic results of clay

ACKNOWLEDGEMENT

The Centre National de la Recherche Scientifique, mainly through Greco Géomatériaux project, is acknowledged for the financial support.

REFERENCES

Golcheh Y. : "Etude de sollicitations rotationnelles sur une kaolinite." Thesis ENTPE: Ecole Centrale de Paris. 1986.

Hicher P.Y., Lade P.v. : "Rotation of principal directions in Ko-consolidated clay." J. Soil Mechanics and Foundations Div, ASCE. 1987. Vol 113, n°7, pp 774-788.

Towhata I., Ishihara K. : "Undrained strength of sand undergoing cyclic rotation of principal stress axes " Soils and Foundations. 1985, n° 2, pp 135-147.

Kharchafi M. ; "Contribution à l'étude du comportement des matériaux granulaires sous sollicitations rotationnelles." Thesis ENTPE: Ecole Centrale de Paris. 1988.

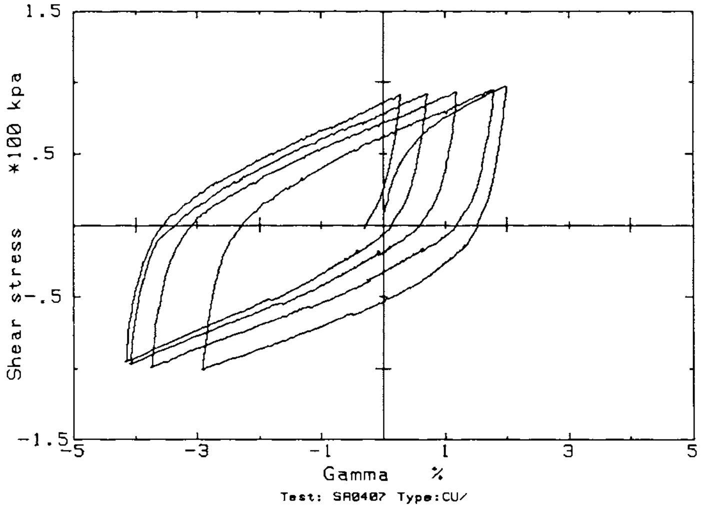

Figure 2a: Cyclic results of Hostun RF

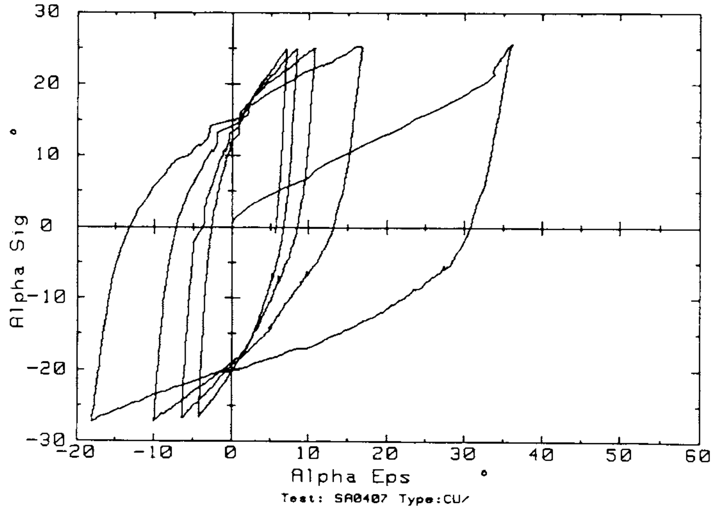

Figure 2c: Cyclic results of Hostun RF

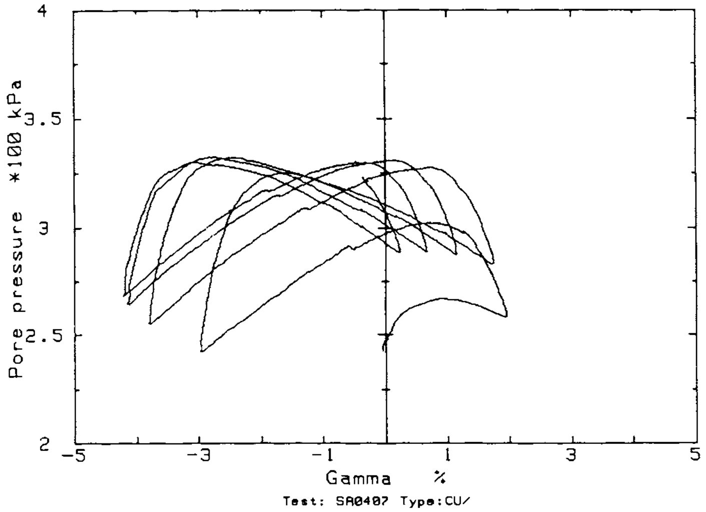

Figure 2b: Cyclic results of Hostun RF

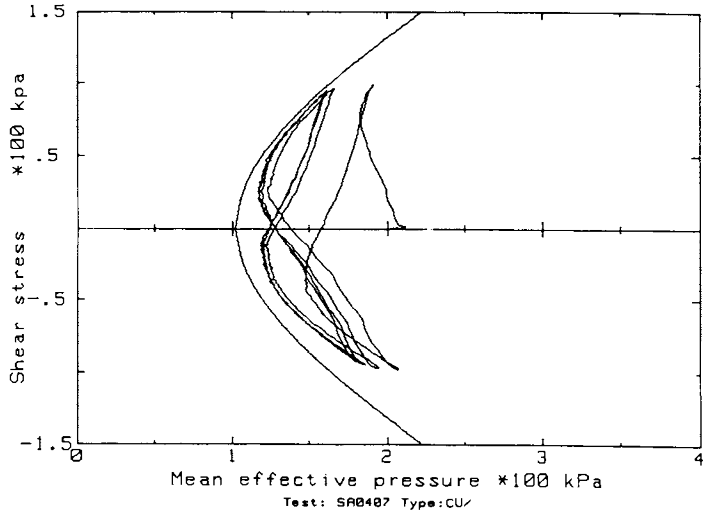

Figure 2d: Cyclic results of Hostun RF

NOTATIONS

τ	torsional shear stress
σ_a	axial stress
σ_θ	circumferential stress
$\sigma_a-\sigma_\theta$	axial deviator
p'	mean effective pressure
σ_c'	effective consolidation stress
γ	distorsion
ε_a	axial strain
ε_θ	circumferential strain
α_σ	rotation of principal stress axes
α_ε	rotation of principal strain axes